

**RI 8906**

PLEASE DO NOT REMOVE FROM LIBRARY

Bureau of Mines Report of Investigations/1984

# Electrochemical Determination of Thermodynamic Properties of Bismuth Sesquioxide and Stannic Oxide

By Seth C. Schaefer



UNITED STATES DEPARTMENT OF THE INTERIOR

**Report of Investigations 8906**

**Electrochemical Determination  
of Thermodynamic Properties  
of Bismuth Sesquioxide  
and Stannic Oxide**

**By Seth C. Schaefer**



**UNITED STATES DEPARTMENT OF THE INTERIOR  
William P. Clark, Secretary**

**BUREAU OF MINES  
Robert C. Horton, Director**

Library of Congress Cataloging in Publication Data:

Schaefer, Seth C

Electrochemical determination of thermodynamic properties of bismuth sesquioxide and stannic oxide.

(Report of investigations / United States Department of the Interior, Bureau of Mines ; 8906)

Supt. of Docs. no.: I 28,23:8906.

Bibliography: p. 14-15.

1. Bismuth trioxide--Thermal properties. 2. Stannic oxide--Thermal properties. 3. Electrochemistry. I, Title. II, Series: Report of investigations (United States. Bureau of Mines) ; 8906.

TN23,U43 [QD181.B5] 622s [546'.7182] 84-600 126

## CONTENTS

	<u>Page</u>
Abstract.....	1
Introduction.....	2
Experimental work.....	3
Materials.....	3
Apparatus and procedure.....	3
Results and discussion.....	5
Bi <sub>2</sub> O <sub>3</sub> .....	5
SnO <sub>2</sub> .....	9
Summary and conclusions.....	13
References.....	14

## ILLUSTRATIONS

1. High-temperature galvanic cell.....	4
2. Emf (E) versus temperature for $2\text{Bi}(\ell) + 3\text{Cu}_2\text{O}(\text{c}) = \text{Bi}_2\text{O}_3(\text{c}) + 6\text{Cu}(\text{c})$ .....	5
3. Equilibrium diagram for Bi-Bi <sub>2</sub> O <sub>3</sub> -O <sub>2</sub> system.....	7
4. Emf (E) versus temperature for $\text{Sn}(\ell) + 2\text{Cu}_2\text{O}(\text{c}) = \text{SnO}_2(\text{c}) + 4\text{Cu}(\text{c})$ .....	11
5. Equilibrium diagram for Sn-SnO <sub>2</sub> -O <sub>2</sub> system.....	11

## TABLES

1. Impurities detected in reagents.....	4
2. Emf (E) of cells W, Bi( $\ell$ ), Bi <sub>2</sub> O <sub>3</sub> ( $\alpha, \delta$ )/ZrO <sub>2</sub> //Cu <sub>2</sub> O, Cu, Pt.....	6
3. Thermodynamic data for $2\text{Bi}(\ell) + 1.5 \text{O}_2(\text{g}) = \text{Bi}_2\text{O}_3(\alpha, \delta, \ell)$ .....	7
4. Standard Gibbs energy change ( $-\Delta G^\circ$ ) for $2\text{Bi}(\ell) + 1.5 \text{O}_2(\text{g}) = \text{Bi}_2\text{O}_3(\alpha, \delta, \ell)$ .....	7
5. X-ray diffraction analyses of samples for Bi <sub>2</sub> O <sub>3</sub> cell.....	8
6. Emf (E) of cells Pt, SnO <sub>2</sub> (junction), Sn( $\ell$ ), SnO <sub>2</sub> //ZrO <sub>2</sub> //Cu <sub>2</sub> O, Cu, Pt....	10
7. Thermodynamic data for $\text{Sn}(\ell) + \text{O}_2(\text{g}) = \text{SnO}_2(\text{c})$ .....	12
8. Standard Gibbs energy change ( $-\Delta G^\circ$ ) for $\text{Sn}(\ell) + \text{O}_2(\text{g}) = \text{SnO}_2(\text{c})$ .....	12
9. X-ray diffraction analyses of samples for SnO <sub>2</sub> cell.....	12

UNIT OF MEASURE ABBREVIATIONS USED IN THIS REPORT

Å	angstrom	K	kelvin
atm	atmosphere	kcal/mol	kilocalorie per mol
at. pct	atomic percent	min	minute
cal	calorie	mm	millimeter
cal/mV	calorie per millivolt	mV	millivolt
cm <sup>3</sup> /min	cubic centimeter per minute	Pa	pascal
h	hour	wt pct	weight percent

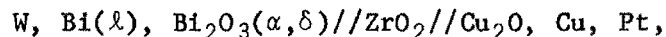
# ELECTROCHEMICAL DETERMINATION OF THERMODYNAMIC PROPERTIES OF BISMUTH SESQUIOXIDE AND STANNIC OXIDE

By Seth C. Schaefer<sup>1</sup>

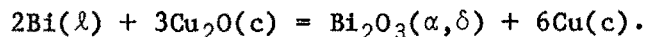
---

## ABSTRACT

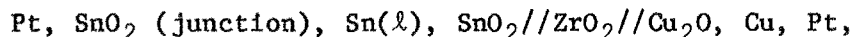
The Bureau of Mines investigated the thermodynamic properties of  $\text{Bi}_2\text{O}_3$  (bismuth sesquioxide) and  $\text{SnO}_2$  (stannic oxide). Standard Gibbs energies of formation ( $\Delta G_f^\circ$ ) of these compounds were determined with high-temperature electromotive force (emf) cells using stabilized  $\text{ZrO}_2$  (zirconia) as the electrolyte. Potential measurements were obtained from the cell



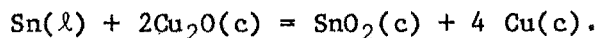
with the overall cell reaction



Similar measurements were obtained for the cell



with the overall cell reaction



Equilibrium oxygen pressures for the  $\text{Bi-Bi}_2\text{O}_3\text{-O}_2$  system were measured and are expressed as

$$\log p_{\text{O}_2} = -20,267/T + 10.20 \quad (740.2\text{-}975.7 \text{ K})$$

and

$$\log p_{\text{O}_2} = -18,534/T + 8.42 \quad (1,017.4\text{-}1,080.5 \text{ K}),$$

where pressure ( $p_{\text{O}_2}$ ) is in atmospheres and temperature (T) is in kelvins. Similarly, equilibrium oxygen pressures for the  $\text{Sn-SnO}_2\text{-O}_2$  system are expressed as

$$\log p_{\text{O}_2} = -30,258/T + 10.99 \quad (814.6\text{-}1,236.6 \text{ K}).$$

---

<sup>1</sup>Metallurgist, Albany Research Center, Bureau of Mines, Albany, OR.

Standard Gibbs energies of formation of  $\text{Bi}_2\text{O}_3$  and  $\text{SnO}_2$  were derived from these measurements and auxiliary data from the literature. The results are expressed as follows:

$$\Delta G_f^\circ(\text{Bi}_2\text{O}_3, \alpha) = (-139.100 + 69.99 \times 10^{-3}T) \pm 0.603 \text{ kcal/mol} \quad (740.2-975.7 \text{ K}),$$

$$\Delta G_f^\circ(\text{Bi}_2\text{O}_3, \delta) = (-127.210 + 57.78 \times 10^{-3}T) \pm 0.606 \text{ kcal/mol} \quad (1,017.4-1,080.5 \text{ K}),$$

and

$$\Delta G_f^\circ(\text{SnO}_2) = (-138.450 + 50.28 \times 10^{-3}T) \pm 0.415 \text{ kcal/mol} \quad (814.6-1,236.6 \text{ K}).$$

The standard enthalpies of formation of  $\text{Bi}_2\text{O}_3$ , and  $\text{SnO}_2$ , derived by the third-law method, are

$$\Delta H_f^\circ_{298}(\text{Bi}_2\text{O}_3, \alpha) = -135.697 \pm 0.603 \text{ kcal/mol}$$

and

$$\Delta H_f^\circ_{298}(\text{SnO}_2) = -137.462 \pm 0.450 \text{ kcal/mol}.$$

## INTRODUCTION

Thermodynamic properties of  $\text{Bi}_2\text{O}_3$  and  $\text{SnO}_2$  were investigated by the Bureau of Mines as a part of its program to expand the base of scientific information needed to devise innovative technologies. Bismuthite ( $\text{Bi}_2\text{O}_3$ ) and bismuthinite ( $\text{Bi}_2\text{S}_3$ ) are the most common bismuth minerals; they are generally associated with lead and copper minerals. Bismuth is recovered as a byproduct during the extraction and refining of lead and copper. Bismuth is used in pharmaceutical products, as catalysts for plastic manufacture, in ferrous and aluminum industries to improve machinability, as an aid to casting iron, and in production of low-melting-point fusible alloys for fire-extinguishing systems.

The only mineral of commercial importance as a source of tin is cassiterite ( $\text{SnO}_2$ ) (1).<sup>2</sup> Cassiterite is usually found in placer and eluvial deposits. In placer deposits, cassiterite is relatively free of impurities because it has greater resistance to weathering than do the minerals originally associated with it. Tin is used in coatings for steel cans, in solders for joining pipes or electrical conductors, and in alloys for widely diversified applications. Although some of the demand for tin in the United States is satisfied by secondary scrap metal, most of the tin requirements are met by imports from Malaysia, Thailand, Boliva, and Indonesia.

Results of numerous investigations of the  $\text{Bi-Bi}_2\text{O}_3\text{-O}_2$  system (2-14) have been reported in the literature; however, inspection of these data shows considerable disagreement in the thermodynamic properties of  $\text{Bi}_2\text{O}_3$  at high temperatures. Comparisons of the enthalpies of the phase transition ( $\alpha$ - $\delta$ ) and fusion ( $\delta$ - $\ell$ ) show large disparities, even in data by different authors using essentially the same technique. Variations in the results are probably related to experimental difficulties that are caused by the corrosive nature (2) of the high-temperature ( $\delta$ ) phase and molten  $\text{Bi}_2\text{O}_3$ , in addition to the hysteresis effects that are prevalent in the ( $\alpha$  to  $\delta$ ) phase transition during heating and cooling cycles. Consequently, accurate measurements of thermodynamic properties are difficult to obtain at high temperatures.

---

<sup>2</sup>Underlined numbers in parentheses refer to items in the list of references at the end of this report.

Thermodynamic properties of the Sn-SnO<sub>2</sub>-O<sub>2</sub> system have previously been investigated by calorimetry (15-16), gas equilibration (17), and emf (18-21) techniques. Results from combustion calorimetry are subject to error because incomplete oxidation of Sn to SnO<sub>2</sub> complicates analyses of the mixed reaction products. Difficulties in achieving equilibrium gas composition at the reaction site lead to erroneous results from gas equilibration techniques that fix the oxygen pressure in a flow system. Emf measurements are complicated by corrosion of the ZrO<sub>2</sub> electrolyte and also at the junction of the liquid Sn + SnO<sub>2</sub> electrode. Selection of an inert junction is required to obtain accurate open-circuit potentials for the cell reaction. The emf method used by the Bureau was designed to obtain accurate equilibrium dissociation pressures of metal-metal oxide systems. This method permits direct determination of the thermodynamic stability of these systems and Gibbs energies of formation of oxides from the elements at high temperatures.

Application of stabilized ZrO<sub>2</sub> as a selective solid-anion electrolyte has been demonstrated in determining Gibbs energies for cell reactions involving metal-metal oxide systems at elevated temperatures (22). Within the limitation of the ionic domain of stabilized ZrO<sub>2</sub>, any equilibrium involving oxygen may be investigated by this technique (23). The method is based on the measurement of the difference in chemical potential between the known oxygen potential of the reference electrode and the oxygen potential of the electrode to be determined. In this investigation, the difference was measured between the oxygen potential of a reference electrode consisting of a 1:1 molar mixture of Cu + Cu<sub>2</sub>O and the oxygen potential of an electrode consisting of a 1:1 molar mixture of Bi + Bi<sub>2</sub>O<sub>3</sub> or Sn + SnO<sub>2</sub>. The standard states are the saturated coexisting phases. The transference number of oxygen is essentially unity in the range of oxygen potential of this investigation (23). The relationship between the open-circuit potential of the cell and the Gibbs energy change for the actual cell reaction is

$$\Delta G(\text{reaction}) = -nFE, \quad (1)$$

where  $\Delta G$  is the change in Gibbs energy for the cell reaction,  $n$  is the number of electrochemical equivalents in the reaction,  $F$  is the Faraday constant (23.061 cal/mV equivalent), and  $E$  is the emf in millivolts.

## EXPERIMENTAL WORK

### Materials

High-purity reagents were obtained from commercial sources and used without further purification. Analyses of these reagents were confirmed and are presented in table 1. Ultra-high-purity argon was passed through Mg(ClO<sub>4</sub>)<sub>2</sub> (magnesium perchlorate) and purified of residual oxygen by passing over hot titanium-zirconium chips to provide an inert atmosphere in the cell for the electrodes.

### Apparatus and Procedure

Internal arrangement of the cell components is illustrated in figure 1. The apparatus, potentiometer, and standardized thermocouple have been described in previous publications (24). The reference electrode was a 1:1 molar mixture of Cu plus Cu<sub>2</sub>O and the electrode of unknown oxygen potential consisted of a 1:1 molar mixture of Bi and Bi<sub>2</sub>O<sub>3</sub> for the Bi<sub>2</sub>O<sub>3</sub> determination or a 1:1 molar mixture of Sn and SnO<sub>2</sub> for the SnO<sub>2</sub> determination. The cell was purged with argon and then evacuated before being backfilled with argon. Flow rate of the argon was approximately 15 cm<sup>3</sup>/min, and a positive pressure of approximately 30 Pa was maintained throughout

TABLE 1. - Impurities detected in reagents

Reagent and impurity elements <sup>1</sup>	wt pct	Reagent and impurity elements <sup>1</sup>	wt pct	Reagent and impurity elements <sup>1</sup>	wt pct
Sn:		Cu:		Bi <sub>2</sub> O <sub>3</sub> :	
Ca.....	0.05	Al.....	<0.01	B.....	0.001
Cu.....	.0002	H.....	.0033	Ca.....	.05
Fe.....	.005	O.....	.0913	Fe.....	.005
Mg.....	.0005	Si.....	<.01	Mg.....	.0005
Pb.....	.05	Bi:		Pb.....	.05
Zn.....	.03	Cu.....	.0002	Si.....	.002
SnO <sub>2</sub> :		Fe.....	.003	Cu <sub>2</sub> O:	
Ca.....	.05	Pb.....	<.005	B.....	<.003
Fe.....	.005			Fe.....	<.01
Pb.....	.03			Ni.....	<.03

<sup>1</sup>Impurities not detected by spectrochemical analyses, except as noted in the table, were Ag, Al, As, B, Ba, Be, Bi, Ca, Cb, Cd, Co, Cr, Cu, Fe, Hf, Li, Mg, Mn, Mo, Na, Ni, P, Pb, Sb, Si, Sn, Ta, Ti, V, W, Zn, and Zr.

the entire experiment. The emf measurements were made with a Keithley<sup>3</sup> model 642 high-input impedance digital electrometer. The cells were heated to approximately 1,000 K and permitted to stabilize for 12 h. Reversibility of the cell reactions was checked by approaching equilibrium from temperatures above and below a specified temperature. Cell response to temperature change was rapid, and potentials stabilized within 1 h after steady-state temperature was obtained. Measurements were obtained over a period of 2 days and repeated two or three times before the cell was dismantled and the electrodes were removed for X-ray analyses. Reproducibility was checked by obtaining measurements from several cells for each determination. Preliminary tests established that tungsten was a satisfactory material to contact the Bi(l) + Bi<sub>2</sub>O<sub>3</sub> electrode at temperatures up to 1,080 K, but it became embrittled after prolonged exposure at higher temperatures. Other materials tested, including Pt, Fe, Mo, Ta, Re, and Nichrome, were either dissolved or severely corroded by liquid bismuth. No stable or reproducible potentials could be obtained. Consequently, investigation of Bi<sub>2</sub>O<sub>3</sub> was limited to the  $\alpha$ - and  $\delta$ -phases in the temperature range 740.2 to 1,080.5 K, and no measurements were obtained for the liquid Bi<sub>2</sub>O<sub>3</sub> phase. Measurements were made to determine the platinum-tungsten thermocouple effect, and appropriate corrections were applied to all emf measurements for the Bi<sub>2</sub>O<sub>3</sub> determination. Corrosion problems at the junction of Sn(l) + SnO<sub>2</sub> were resolved by using SnO<sub>2</sub> that was compacted into a cylinder 10 mm long and 4 mm in diameter. These compacts were sintered at 1,200 K, and a platinum extension wire was attached to the top of the SnO<sub>2</sub> compact.

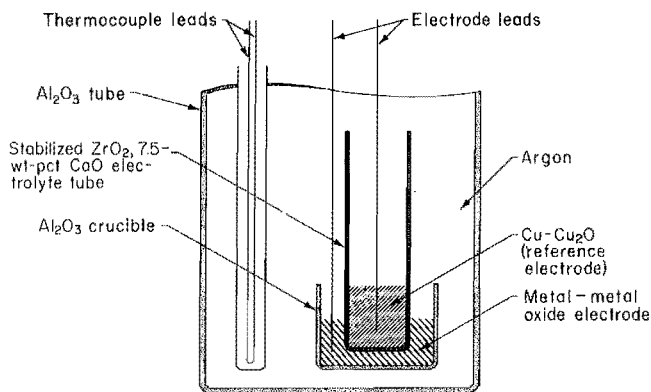


FIGURE 1. - High-temperature galvanic cell.

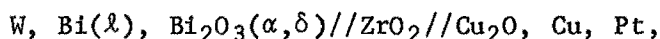
<sup>3</sup>Reference to specific trade names does not imply indorsement by the Bureau of Mines.

Only the  $\text{SnO}_2$  was immersed in the  $\text{Sn}(\ell) + \text{SnO}_2$  electrode.  $\text{SnO}_2$  is an electronic conductor under the conditions of this investigation (25). Resistance of this junction decreases with increasing temperature and decreasing oxygen pressure. Measurements were made to determine the Pt- $\text{SnO}_2$ -Pt junction potential, and these corrections were applied to all emf measurements for the  $\text{SnO}_2$  determination.

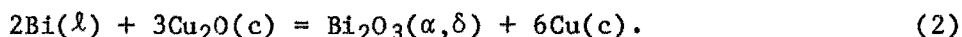
## RESULTS AND DISCUSSION

### $\text{Bi}_2\text{O}_3$

The equilibrium oxygen pressure for the  $\text{Bi-Bi}_2\text{O}_3\text{-O}_2$  system and the standard Gibbs energy of formation of  $\text{Bi}_2\text{O}_3$  were determined by measuring the potentials of the reversible galvanic cell



with the overall cell reaction



Potential measurements from three cells that were used for the  $\text{Bi}_2\text{O}_3$  determination are given in table 2. These results may be expressed as a function of temperature by the least squares equation and standard error of estimate as follows:

$$E = (135.326 - 0.132234T) \pm 0.46 \quad (740.2-975.7 \text{ K}) \quad (3)$$

$$\text{and} \quad E = (49.396 - 0.044001T) \pm 0.61 \quad (1,017.4-1,080.5 \text{ K}), \quad (4)$$

where  $E$  is emf expressed in millivolts. Smooth emf data derived from equations 3 and 4 are given in columns 4 and 8 of table 2. Representative emf-versus-temperature data are illustrated in figure 2.

The equilibrium oxygen pressure,  $p\text{O}_2$ , over  $\text{Bi}(\ell) + \text{Bi}_2\text{O}_3$  is determined from the potential measurements for cell reaction 2 and may be expressed as

$$\begin{aligned} \text{O}_2'(\text{g, over Cu} + \text{Cu}_2\text{O}) \\ = \text{O}_2(\text{g, over Bi}(\ell) + \text{Bi}_2\text{O}_3). \end{aligned} \quad (5)$$

The corresponding standard Gibbs energy change,  $\Delta G^\circ$ , for reaction 5 is

$$\begin{aligned} \Delta G^\circ(\text{reaction 5}) &= -nFE \\ &= RT \ln p\text{O}_2 - RT \ln p\text{O}_2', \end{aligned} \quad (6)$$

where  $n$  is 4,  $F$  is the Faraday constant,  $E$  is the emf from equation 3 or 4, and  $p\text{O}_2'$  is the oxygen pressure over the reference electrode ( $\text{Cu} + \text{Cu}_2\text{O}$ ). Pressures are expressed in atmospheres. In the temperature range 800 to 1,200 K, the standard Gibbs energy of  $\text{Cu}_2\text{O}$  derived from a critical analysis of all published data (26) is expressed as

$$\begin{aligned} \Delta G_f^\circ(\text{Cu}_2\text{O}) &= (-40.125 + \\ &17.23 \times 10^{-3}T) \pm 0.200 \text{ kcal/mol,} \end{aligned} \quad (7)$$

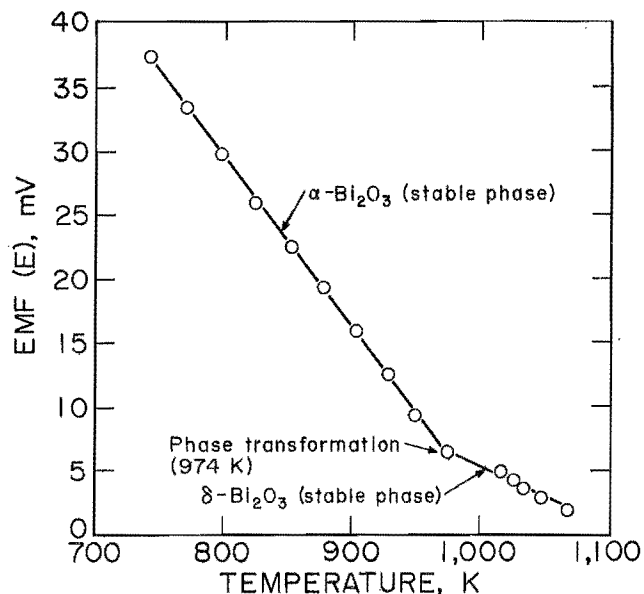


FIGURE 2. - Emf ( $E$ ) versus temperature for  $2\text{Bi}(\ell) + 3\text{Cu}_2\text{O}(\text{c}) = \text{Bi}_2\text{O}_3(\text{c}) + 6\text{Cu}(\text{c})$ .

TABLE 2. - Emf (E) of cells W, Bi(l), Bi<sub>2</sub>O<sub>3</sub>( $\alpha,\delta$ )/ZrO<sub>2</sub>/Cu<sub>2</sub>O, Cu, Pt

Measurement	Temperature, K	Emf (E), mV		Measurement	Temperature, K	Emf (E), mV	
		Measured <sup>1</sup>	Calculated <sup>2</sup>			Measured <sup>1</sup>	Calculated <sup>2</sup>
1.....	740.2	37.18	37.45	23.....	927.0	12.26	12.75
2.....	742.3	36.21	37.17	24.....	927.2	12.56	12.72
3.....	742.4	37.49	37.16	25.....	928.2	12.48	12.59
4.....	769.0	33.50	33.64	26.....	950.5	9.42	9.64
5.....	771.1	33.62	33.36	27.....	951.5	9.23	9.51
6.....	771.5	32.52	33.31	28.....	952.1	9.22	9.43
7.....	797.7	29.88	29.84	29.....	974.8	6.43	6.42
8.....	798.0	30.35	29.80	30.....	975.1	6.55	6.39
9.....	799.1	29.18	29.66	31.....	975.7	6.23	6.31
10.....	825.3	26.54	26.19	32.....	1,017.4	5.12	4.63
11.....	825.6	26.85	26.15	33.....	1,027.4	4.21	4.19
12.....	827.2	25.90	25.94	34.....	1,036.0	3.61	3.81
13.....	851.8	23.57	22.69	35.....	1,045.8	2.96	3.38
14.....	852.3	23.15	22.62	36.....	1,046.1	4.28	3.36
15.....	854.3	22.41	22.36	37.....	1,050.8	3.03	3.16
16.....	876.4	19.23	19.44	38.....	1,053.9	2.45	3.02
17.....	878.5	19.25	19.16	39.....	1,059.9	2.41	2.75
18.....	879.1	20.20	19.08	40.....	1,064.0	1.85	2.57
19.....	902.7	15.72	15.96	41.....	1,068.7	1.81	2.37
20.....	903.0	15.50	15.92	42.....	1,075.1	2.74	2.09
21.....	903.9	15.62	15.80	43.....	1,080.5	2.69	1.85
22.....	904.5	15.91	15.72				

<sup>1</sup>Average of 2 measurements ( $\pm 0.005$  mV) taken at 20-min intervals and corrected for cell calibration and W-Pt thermocouple potential.

<sup>2</sup>Calculated from equations

$$E = (135.326 - 0.132234T) \pm 0.46 \quad (740.2-975.7 \text{ K})$$

and

$$E = (49.396 - 0.044001T) \pm 0.61 \quad (1,017.4-1,080.5 \text{ K}).$$

and the dissociation pressure of oxygen,  $pO_2$ , over Cu + Cu<sub>2</sub>O in equation 5 may be expressed as

$$\log pO_2 = -17,539/T + 7.53121. \quad (8)$$

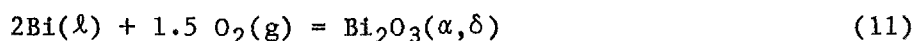
Rearranging equation 6 and substituting values of  $pO_2$  from equation 8 and E from equation 3 or 4 yields

$$\log pO_2 = -20,267/T + 10.20 \quad (740.2-975.7 \text{ K}) \quad (9)$$

and

$$\log pO_2 = -18,534/T + 8.42 \quad (1,017.4-1,080.5 \text{ K}). \quad (10)$$

Figure 3 illustrates the thermodynamic stability of the Bi-Bi<sub>2</sub>O<sub>3</sub>-O<sub>2</sub> system in the temperature range 740.2 to 1,080.5 K. A phase transition ( $\alpha$ - $\delta$ ) of Bi<sub>2</sub>O<sub>3</sub> was detected at 974 K. Reaction 5 and equation 6 are independent relationships that are applicable to any equilibrium involving oxygen. These values of  $pO_2$  at the reaction site are the key for computing the standard Gibbs energy change for the reaction



from the relationship

$$\begin{aligned}\Delta G^\circ(\text{reaction 11}) &= -RT \ln K_{11} \\ &= 1.5RT \ln pO_2,\end{aligned}\quad (12)$$

where  $K_{11}$  is the equilibrium constant for reaction 11, and the condensed phases are assumed to have unit activity. Linear equations expressing the oxygen pressures and the corresponding standard Gibbs energy change for reaction 11 are given in table 3. Results at specified temperatures from this investigation together with those of previous investigators are given in table 4. Agreement is favorable in the temperature range 800 to 900 K for  $\alpha$ - $Bi_2O_3$ ; however, variation in the results becomes more evident at higher temperatures and is probably attributable to the side reactions of the high-temperature ( $\delta$ ) and liquid  $Bi_2O_3$  phases with the containers or cell components.

X-ray diffraction analyses of electrode products are given in table 5. The

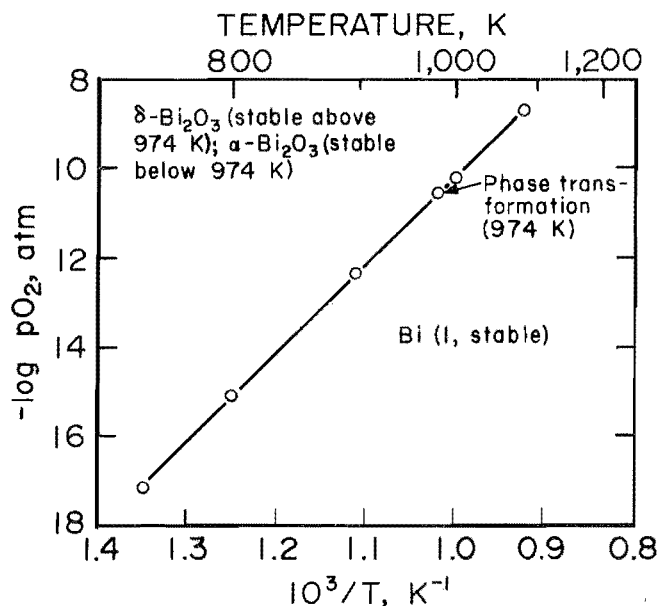


FIGURE 3. - Equilibrium diagram for  $Bi-Bi_2O_3-O_2$  system.

TABLE 3. - Thermodynamic data for  $2Bi(l) + 1.5 O_2(g) = Bi_2O_3(\alpha, \delta, l)$

Method	Temperature range, K	log $pO_2$ , atm	Standard Gibbs energy change, cal <sup>1</sup>		Reference
			$\Delta H^\circ$	$-\Delta S^\circ$	
Emf.....	740.2- 975.7	-20,267/T+10.20	-139,100	69.99	This work.
	1,017.4-1,080.5	-18,534/T+ 8.42	-127,210	57.78	Do.
	885 - 991	-20,928/T+10.98	-143,640	75.34	Mehrotra (12).
	991 -1,095	-19,420/T+ 9.45	-133,290	64.89	Do.
	1,095 -1,223	-17,373/T+ 7.58	-119,240	52.05	Do.
	793 -1,093	-19,508/T+ 9.24	-133,890	63.43	Chatterji (4).
	773 - 973	-21,925/T+11.65	-150,480	79.94	Rao (13).
	1,073 -1,223	-14,468/T+ 4.52	-99,300	31	Hahn (7).
	949 -1,076	-19,626/T+ 9.32	-134,700	64	Cahen (3).
	1,003 -1,098	-19,591/T+ 8.81	-134,461	60.49	Siderov (14).
Mass spectrometric...	1,100 -1,193	-18,810/T+ 8.10	-129,101	55.61	Do.
	545 -1,003	-20,234/T+10.03	-139,559	68.85	Pankratz (26).
Calorimetry.....	1,003 -1,098	-19,079/T+ 8.78	-130,950	60.26	Do.
	1,098 -1,300	-18,340/T+ 8.11	-125,877	55.64	Do.

$${}^1\Delta G^\circ(\text{reaction}) = \Delta H^\circ - T\Delta S^\circ.$$

TABLE 4. - Standard Gibbs energy change ( $-\Delta G^\circ$ ) for  $2Bi(l) + 1.5 O_2(g) = Bi_2O_3(\alpha, \delta, l)$ , kcal/mol  $Bi_2O_3$

Temperature, K	Phase <sup>1</sup>	Mehrotra(12)	Chatterji(4)	Rao(13)	Hahn(7)	Cahen(3)	Siderov(14)	Pankratz(26)	This work
740.2	$\alpha$	ND	ND	ND	ND	ND	ND	88.693	87.293
800	$\alpha$	ND	83.146	86.528	ND	ND	ND	84.483	83.108
900	$\alpha$	75.834	76.803	78.534	ND	ND	ND	77.574	76.109
1,000	$\delta$	68.400	70.460	ND	ND	70.700	73.971	70.714	69.430
1,100	$l$	61.985	ND	ND	65.200	ND	67.930	64.671	ND
1,200	$l$	56.780	ND	ND	62.100	ND	62.369	59.108	ND

ND Not determined.

<sup>1</sup>Phase transition ( $\alpha$  to  $\delta$ ) detected at 974 K;  $\Delta H$  transition = 11.890 kcal/mol.

TABLE 5. - X-ray diffraction analyses of samples for Bi<sub>2</sub>O<sub>3</sub> cell

Sample	Phase identified	Crystal structure	Parametric measurements <sup>1</sup>				Card <sup>2</sup>
			a <sub>o</sub>	b <sub>o</sub>	c <sub>o</sub>	β	
Reagents:							
Cu.....	Cu.....	Cubic.....	3.615	NAp	NAp	NAp	4-836
Cu <sub>2</sub> O.....	Cu <sub>2</sub> O....	...do.....	4.2696	NAp	NAp	NAp	5-667
Bi.....	Bi.....	Hexagonal.....	4.546	NAp	11.860	NAp	5-0519
Bi <sub>2</sub> O <sub>3</sub> .....	Bi <sub>2</sub> O <sub>3</sub> ...	Monoclinic.....	5.848	8.166	7.510	113	27-53
Electrodes:							
Cathode.....	Cu.....	Cubic.....	3.613 ± 0.001	NAp	NAp	NAp	4-836
	Cu <sub>2</sub> O....	...do.....	4.268 ± .001	NAp	NAP	NAp	5-667
Anode.....	Bi.....	Hexagonal.....	4.5455 ± .0009	NAp	11.861 ± 0.002	NAp	5-0519
	Bi <sub>2</sub> O <sub>3</sub> ...	Monoclinic.....	5.854 ± .003	8.187 ± 0.005	7.518 ± .004	112.86 ± 0.001	27-53

NAp Not applicable.

<sup>1</sup>Parametric measurements--a<sub>o</sub>, b<sub>o</sub>, and c<sub>o</sub> expressed in angstroms (Å) and β expressed in degree (°)--for reagents were obtained from the literature.

<sup>2</sup>Numbers refer to data file cards of Joint Committee of Powder Diffraction Standards, International Centre of Diffraction Data, Swarthmore, PA.

results showed no major change in lattice parameters between the reagents and the components in the equilibrated electrode mixtures. The lattice parameter of a solid solution generally changes with the composition up to the saturation limit and then remains constant beyond that point. Solubilities of oxygen in copper have been reported as 0.0018 and 0.0136 at. pct at 1,073 and 1,250 K, respectively (27). Maximum solubilities of oxygen in liquid bismuth have been reported as 0.0151 and 0.0341 at. pct at 1,073 and 1,223 K (28). Consequently, the intersolubility is negligible, and the assumption of unit activity for the reactants and products does not introduce any appreciable error in the Gibbs energy of formation of Bi<sub>2</sub>O<sub>3</sub> in the temperature range of this investigation. The standard Gibbs energy of formation of Bi<sub>2</sub>O<sub>3</sub> may also be determined from the cell potentials of reaction 2 and the relationship

$$\Delta G^\circ(\text{reaction 2}) = -nFE = \Delta G_f^\circ(\text{Bi}_2\text{O}_3) - 3\Delta G_f^\circ(\text{Cu}_2\text{O}). \quad (13)$$

In equation 13, n is equal to 6. Rearranging equation 13 and substituting the value of E from equation 3 or 4, and the standard Gibbs energy of formation of Cu<sub>2</sub>O as given in equation 7, yields

$$\Delta G_f^\circ(\text{Bi}_2\text{O}_3, \alpha) = (-139.100 + 69.99 \times 10^{-3}T) \pm 0.603 \text{ kcal/mol (740.2-975.7 K)} \quad (14)$$

and

$$\Delta G_f^\circ(\text{Bi}_2\text{O}_3, \delta) = (-127.210 + 57.78 \times 10^{-3}T) \pm 0.606 \text{ kcal/mol (1,017.4-1,080.5 K)}. \quad (15)$$

Equations 14 and 15 are identical to the results derived from equation 12 and given in columns 4 and 5 of table 3. This is to be expected because the standard Gibbs energy of formation of Cu<sub>2</sub>O is involved in both methods for resolution of the Gibbs energy of formation of Bi<sub>2</sub>O<sub>3</sub>. A phase transformation (α - δ) in Bi<sub>2</sub>O<sub>3</sub> occurs at 974 K. An enthalpy of approximately 11.890 kcal/mol Bi<sub>2</sub>O<sub>3</sub> is associated with this transition. These results compare with enthalpies for this transition of 7.06 (8), 9.9 (9), 10.35 (12), 13.6 (13), and 27.9 (6) kcal/mol, and transition temperatures of

978 K (13), 990±7 (6), 991 (12), and 1,003 (8-9). Discrepancies in these results are probably caused by experimental problems associated with the determination of properties of the high-temperature ( $\text{Bi}_2\text{O}_3, \delta$ ) phase, which were previously discussed.

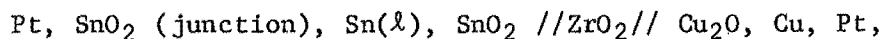
A third-law analysis using equation 14 for the Gibbs energy of formation of ( $\text{Bi}_2\text{O}_3, \alpha$ ) combined with entropy and enthalpy data for Bi (26),  $\text{O}_2$  (26), and  $\text{Bi}_2\text{O}_3$  (26) yields

$$\Delta H_f^\circ_{298} = -135.697 \pm 0.603 \text{ kcal/mol}, \quad (16)$$

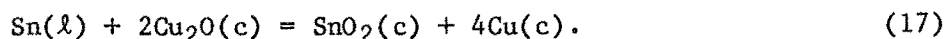
where the standard states are pure crystalline Bi and  $\text{Bi}_2\text{O}_3$ , and gaseous  $\text{O}_2$  at unit fugacity. This value compares favorably with  $-137.160 \pm 0.30$  kcal/mol, which has been reported in the literature (26) and is based on data obtained from combustion calorimetry (11).

### SnO<sub>2</sub>

The equilibrium oxygen pressure for the Sn-SnO<sub>2</sub>-O<sub>2</sub> system and the standard Gibbs energy of formation of SnO<sub>2</sub> were determined by measuring the potentials of the reversible galvanic cell



with the overall cell reaction



Potential measurements from three cells that were used for the SnO<sub>2</sub> determination are given in table 6. These results may be expressed as a function of temperature by the linear equation and standard error of estimate

$$E = (630.94 - 0.17154T) \pm 1.21 \quad (814.6-1,236.6 \text{ K}), \quad (18)$$

where E is emf in millivolts. Potential measurements and their corresponding smooth values derived from equation 18 are given in columns 3, 4, 7, and 8 of table 6. Representative emf-versus-temperature data are illustrated in figure 4.

The equilibrium oxygen pressure,  $p_{\text{O}_2}$ , over Sn( $\ell$ ) + SnO<sub>2</sub> is obtained by the method previously described for reaction 5. Rearranging equation 6 and substituting values of  $p_{\text{O}_2}$  from equation 8 and E from equation 18 yields

$$\log p_{\text{O}_2} = -30,258/T + 10.99 \quad (814.6-1,236.6 \text{ K}). \quad (19)$$

Figure 5 illustrates the thermodynamic stability of the Sn-SnO<sub>2</sub>-O<sub>2</sub> system in the temperature range 814.6 to 1,236.6 K. The standard Gibbs energy change for the reaction



is obtained from the relationship

$$\Delta G^\circ(\text{reaction 20}) = -RT \ln K_{20} = RT \ln p_{\text{O}_2}, \quad (21)$$

TABLE 6. - Emf (E) of cells Pt, SnO<sub>2</sub> (junction), Sn(l), SnO<sub>2</sub>//ZrO<sub>2</sub>//Cu<sub>2</sub>O, Cu, Pt

Measurement	Temperature, K	Emf (E), mV		Measurement	Temperature, K	Emf (E), mV	
		Measured <sup>1</sup>	Calculated <sup>2</sup>			Measured <sup>1</sup>	Calculated <sup>2</sup>
1.....	814.6	492.73	491.20	34.....	1,089.8	443.08	444.00
2.....	842.7	489.05	486.38	35.....	1,108.7	440.79	440.75
3.....	923.3	469.55	472.56	36.....	1,110.0	440.68	440.53
4.....	943.7	472.05	469.06	37.....	1,111.4	439.36	440.29
5.....	948.0	465.40	468.32	38.....	1,129.9	436.98	437.12
6.....	969.0	466.39	464.72	39.....	1,132.0	436.66	436.76
7.....	970.5	462.28	464.46	40.....	1,132.5	437.61	436.67
8.....	971.8	462.27	464.23	41.....	1,133.1	436.35	436.57
9.....	972.7	462.56	464.08	42.....	1,133.3	436.15	436.53
10.....	993.2	462.75	460.57	43.....	1,133.7	436.90	436.46
11.....	994.5	461.14	460.34	44.....	1,133.8	435.55	436.45
12.....	995.2	459.03	460.22	45.....	1,152.1	433.06	433.31
13.....	995.4	458.42	460.19	46.....	1,153.2	432.45	433.12
14.....	1,018.0	457.50	456.31	47.....	1,154.9	433.94	432.83
15.....	1,018.2	454.90	456.28	48.....	1,155.1	432.73	432.79
16.....	1,019.1	455.79	456.12	49.....	1,155.2	432.53	432.78
17.....	1,039.9	451.79	452.55	50.....	1,155.9	433.92	432.66
18.....	1,041.3	453.47	452.31	51.....	1,175.2	430.23	429.35
19.....	1,041.4	450.67	452.30	52.....	1,175.9	428.63	429.23
20.....	1,041.5	452.07	452.28	53.....	1,176.7	428.72	429.09
21.....	1,042.0	453.26	452.19	54.....	1,177.3	428.41	428.99
22.....	1,042.4	452.86	452.13	55.....	1,177.5	430.21	428.95
23.....	1,043.2	450.95	451.99	56.....	1,196.4	425.12	425.71
24.....	1,043.6	452.95	451.92	57.....	1,196.6	426.52	425.68
25.....	1,063.4	448.95	448.52	58.....	1,197.1	425.21	425.59
26.....	1,065.4	448.63	448.18	59.....	1,197.9	426.60	425.45
27.....	1,066.8	446.91	447.94	60.....	1,198.0	424.80	425.44
28.....	1,067.2	448.81	447.87	61.....	1,216.2	423.22	422.31
29.....	1,086.1	444.92	444.63	62.....	1,217.0	421.71	422.18
30.....	1,086.8	444.81	444.51	63.....	1,217.3	421.40	422.12
31.....	1,088.2	444.50	444.27	64.....	1,217.5	423.21	422.09
32.....	1,088.8	443.79	444.17	65.....	1,236.6	418.11	418.81
33.....	1,089.4	445.47	444.06				

<sup>1</sup>Average of 2 measurements ( $\pm 0.05$  mV) taken at 20-min intervals and corrected for cell and junction calibration.

<sup>2</sup>Calculated from linear equation  $E = (630.94 - 0.17154T) \pm 1.21$ .

where  $K_{20}$  is the equilibrium constant for reaction 20, and the condensed phases are assumed to have unit activity. Linear equations, expressing the standard Gibbs energy change for reaction 20, obtained from this study and those derived by previous investigators are given in columns 4 and 5 of table 7. Results at specified temperatures are presented in table 8. Agreement of the results is good considering the experimental difficulties such as the corrosion problems at the junction of the Sn(l) + SnO<sub>2</sub> electrode that were encountered in the emf investigations (18-21), the incomplete oxidation of Sn to SnO<sub>2</sub> by the combustion calorimetry method (15-16), and the uncertainty in achieving equilibrium by the gas-phase equilibrium technique (17). Slight discrepancies in the results are probably caused by side reactions with the containers, impurities in the reagents, and errors in analyses of the combustion products.

X-ray diffraction analyses of electrode products are reported in table 9. The results showed no major change in lattice parameters between the reagents and the components in the equilibrated electrode mixtures. Further evidence concerning the limited intersolubility of the condensed components in the  $\text{Sn}(\ell) + \text{SnO}_2$  electrode is given in the literature (18, 28-29). Consequently, the assumption of unit activity for the condensed phases in reaction 17 does not introduce any appreciable error in the Gibbs energy of formation of  $\text{SnO}_2$  in the temperature range of this investigation. The standard Gibbs energy of formation may also be derived from the cell potential measurements for reaction 17 and the relationship

$$\begin{aligned} \Delta G^\circ(\text{reaction 19}) &= -nFE \\ &= \Delta G_f^\circ(\text{SnO}_2) - 2\Delta G_f^\circ(\text{Cu}_2\text{O}). \end{aligned} \quad (22)$$

In reaction 17,  $n$  is equal to 4,  $F$  is the Faraday constant,  $E$  is from equation 18, and  $\Delta G_f^\circ(\text{Cu}_2\text{O})$  is from equation 7 (26). Rearranging equation 22 and solving for  $\Delta G_f^\circ(\text{SnO}_2)$  yields

$$\begin{aligned} \Delta G_f^\circ(\text{SnO}_2) &= (-138.450 + 50.28 \times 10^{-3}T) \\ &\pm 0.415 \text{ kcal/mol} \quad (814.6-1,236.6 \text{ K}). \end{aligned} \quad (23)$$

Equation 23 is identical to the results from this investigation that were obtained from equation 21 and given in columns 4 and 5 of table 7. Both procedures for resolution of the standard Gibbs energy of  $\text{SnO}_2$  involve the standard Gibbs energy of formation of  $\text{Cu}_2\text{O}$  as given by equation 7.

A third-law analysis of the above Gibbs energy of formation of  $\text{SnO}_2$ , combined with entropy and enthalpy data for  $\text{Sn}$  (26),  $\text{O}_2$  (26), and  $\text{SnO}_2$  (26), yields a standard enthalpy of formation of  $\text{SnO}_2$

$$\Delta H_f^\circ_{298} = -137.462 \pm 0.450 \text{ kcal/mol}, \quad (24)$$

where the standard states are pure crystalline  $\text{Sn}(\beta)$  and  $\text{SnO}_2$ , and gaseous  $\text{O}_2$  at unit fugacity. Close agreement exists with the values  $-138.82 \pm 0.08$  (15) and  $-138.057 \pm 0.038$  (16) kcal/mol, which were the only direct measurements for the standard enthalpy of formation of  $\text{SnO}_2$  by combustion calorimetry.

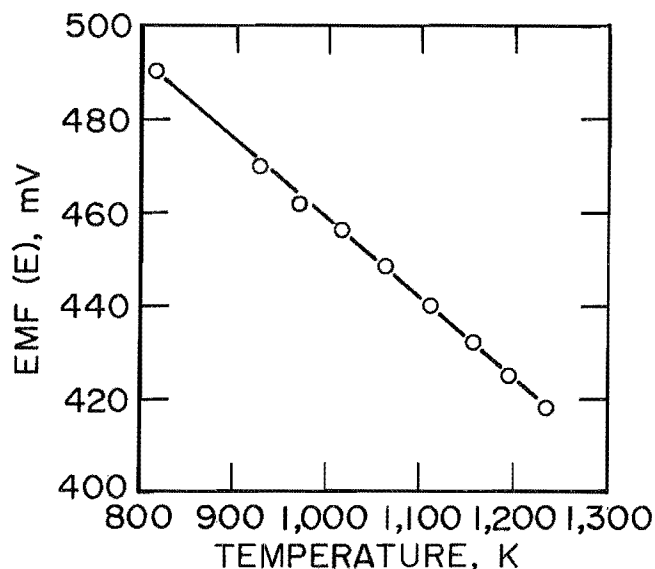


FIGURE 4. - Emf (E) versus temperature for  $\text{Sn}(\ell) + 2\text{Cu}_2\text{O}(\text{c}) = \text{SnO}_2(\text{c}) + 4\text{Cu}(\text{c})$ .

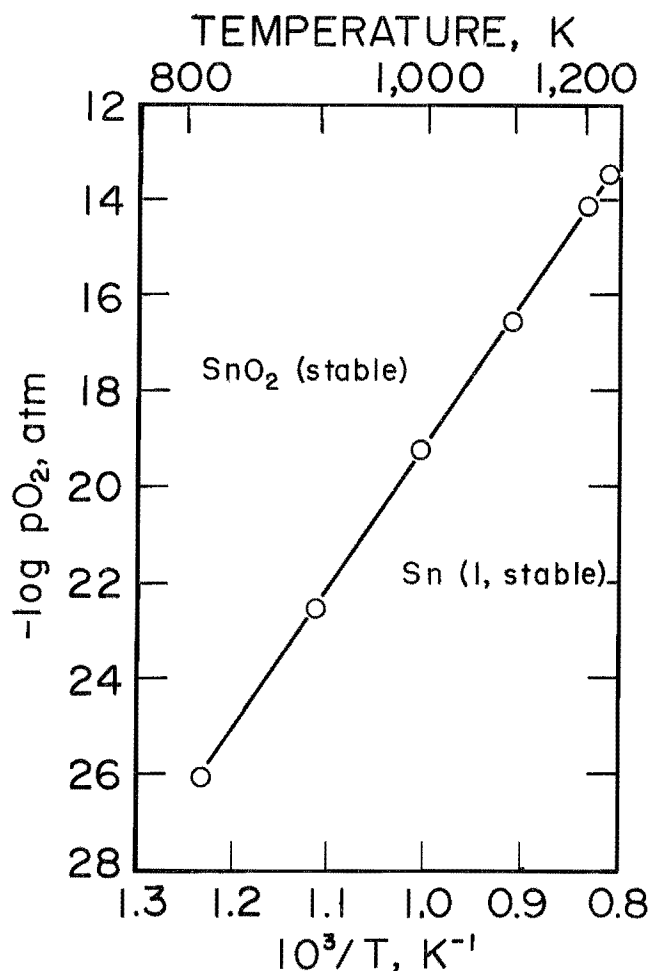


FIGURE 5. - Equilibrium diagram for  $\text{Sn-SnO}_2\text{-O}_2$  system.

TABLE 7. - Thermodynamic data for  $\text{Sn}(\ell) + \text{O}_2(\text{g}) = \text{SnO}_2(\text{c})$ 

Method	Temperature range, K	$\log p\text{O}_2$ , atm	Standard Gibbs energy change, cal <sup>1</sup>		Reference
			$\Delta\text{H}^\circ$	$-\Delta\text{S}^\circ$	
Emf.....	814.6-1,236.6	-30,258/T+10.99	-138,450	50.28	This work.
	773 -1,373	-30,103/T+10.81	-137,738	49.48	Petot-Ervas (19).
	770 - 980	-30,520/T+11.06	-139,650	50.60	Bedford (18).
	990 -1,371	-30,038/T+10.83	-137,444	49.56	Seetharaman (21).
	773 -1,173	-30,115/T+10.18	-137,797	49.77	Ramanarayanan (20)
Gas phase equilibration.....	806 -1,107	-30,312/T+10.99	-138,698	50.28	Platteeuv (17).
Calorimetry.....	ND	-30,324/T+10.77	-138,750	49.28	Humphrey (15).
	ND	-30,158/T+10.77	-137.994	49.28	Lavut (16).

ND Not determined.

$${}^1\Delta\text{G}^\circ(\text{reaction}) = \Delta\text{H}^\circ - \text{T}\Delta\text{S}^\circ.$$

TABLE 8. - Standard Gibbs energy change ( $-\Delta\text{G}^\circ$ ) for  $\text{Sn}(\ell) + \text{O}_2(\text{g}) = \text{SnO}_2(\text{c})$ , kcal/mol  $\text{SnO}_2$ 

Temperature, K	Petot-Ervas(19)	Bedford(18)	Seetharaman(21)	Ramanarayanan(20)	Platteeuv(17)	Humphrey(15)	Lavut(16)	This work
800	98.154	99.170	97.795	97.981	98.474	99.326	98.570	97.486
900	93.206	94.110	92.840	93.004	93.446	93.446	94.398	93.205
1,000	88.258	89.050	87.884	88.027	88.418	89.470	88.714	88.163
1,100	83.310	ND	82.928	83.050	83.390	84.542	83.786	83.134
1,200	78.362	ND	77.972	78.073	ND	79.614	78.858	78.114
1,300	73.414	ND	73.015	ND	ND	74.686	73.930	ND

ND Not determined.

TABLE 9. - X-ray diffraction analyses of samples for  $\text{SnO}_2$  cell

Sample	Phase identified	Crystal structure	Parametric measurements <sup>1</sup>		
			$a_o$	$c_o$	Card <sup>2</sup>
Reagents:					
Cu.....	Cu.....	Cubic.....	3.615	NAP	4-836
$\text{Cu}_2\text{O}$ .....	$\text{Cu}_2\text{O}$ .....	...do.....	4.2696	NAP	5-667
Sn.....	Sn.....	Tetragonal.....	5.831	3.182	4-6739437
$\text{SnO}_2$ .....	$\text{SnO}_2$ .....	...do.....	4.738	3.188	21-1250
Electrodes:					
Cathode.....	Cu.....	Cubic.....	$3.613 \pm 0.001$	NAP	4-836
	$\text{Cu}_2\text{O}$ .....	...do.....	$4.268 \pm .001$	NAP	5-667
Anode.....	Sn.....	Tetragonal.....	$5.830 \pm .003$	$3.182 \pm 0.002$	4-673
	$\text{SnO}_2$ .....	...do.....	$4.735 \pm .001$	$3.18 \pm .003$	21-1250

NAP Not applicable.

<sup>1</sup>Parametric measurements--expressed in angstroms (Å)--for reagents were obtained from the literature.

<sup>2</sup>Numbers refer to data file cards of Joint Committee of Powder Diffraction Standards, International Centre of Diffraction Data, Swarthmore, PA.

## SUMMARY AND CONCLUSIONS

Equilibrium oxygen pressures of the Bi-Bi<sub>2</sub>O<sub>3</sub>-O<sub>2</sub> and Sn-SnO<sub>2</sub>-O<sub>2</sub> systems were measured by a high-temperature emf method using a solid electrolyte tube of stabilized ZrO<sub>2</sub>. The emf measurements yielded standard Gibbs energies of formation of Bi<sub>2</sub>O<sub>3</sub> and SnO<sub>2</sub> from the elements. The enthalpy and temperature for the  $\alpha$  to  $\delta$  phase transformation of Bi<sub>2</sub>O<sub>3</sub> were determined. These data for Bi<sub>2</sub>O<sub>3</sub> and SnO<sub>2</sub> were compared with previously reported measurements, and discrepancies were discussed. Standard enthalpies of formation of Bi<sub>2</sub>O<sub>3</sub> and SnO<sub>2</sub> were derived by combining results from this investigation with auxiliary data from the literature.

## REFERENCES

1. Harris, K. L. Tin. Ch. in Mineral Facts and Problems, Bicentennial Edition. BuMines B 667, 1975, pp. 1127-1141.
2. Anderson, C. T. The Heat Capacities of Bismuth and Bismuth Trioxide at Low Temperatures. J. Am. Chem. Soc., v. 52, 1930, pp. 2720-2723.
3. Cahen, H. T., M. J. Verkerk, and G. H. J. Broers. Gibbs Free Energy of Formation of  $\text{Bi}_2\text{O}_3$  From EMF Cells With  $\delta\text{-Bi}_2\text{O}_3$  Solid Electrolyte. Electrochim. Acta, v. 23, 1978, pp. 885-889.
4. Chatterji, D., and J. V. Smith. Free Energy of Formation of  $\text{Bi}_2\text{O}_3$ ,  $\text{Sb}_2\text{O}_3$ , and  $\text{TeO}_2$  From EMF Measurements. J. Electrochem. Soc., v. 120, 1973, pp. 889-893.
5. Cubicciotti, D., and H. Eding. Enthalpy and Entropy Increments Above 290° K for  $\text{BiBr}_3$ ,  $\text{Bi}_2\text{O}_3$ ,  $\text{Tl}_2\text{O}_3$ , and  $\text{TlO}_2$ . J. Chem. and Eng. Data, v. 12, 1967, pp. 548-551.
6. Gattow, V. G., and H. Schröder. Die Kristallstruktur der Hochtemperaturmodifikation Wismut (III)-oxide ( $\delta\text{-Bi}_2\text{O}_3$ ) (The Crystal Structure of the High-Temperature-Modification of  $\delta\text{-Bi}_2\text{O}_3$ ). Z. Anorg. und Allg. Chem., v. 298, 1962, pp. 176-187.
7. Hahn, S. K., and D. A. Stevenson. Thermodynamic Investigation of Antimony + Oxygen and Bismuth + Oxygen Using Solid-State Electrochemical Techniques. J. Chem. Thermodyn., v. 11, 1979, pp. 627-637.
8. Harwig, H. A., and A. G. Gerards. The Polymorphism of Bismuth Sesquioxide. Thermochim. Acta, v. 28, 1979, pp. 121-131.
9. Levin, E. M., and C. L. McDaniel. Heats of Transformations in Bismuth Oxide by Differential Thermal Analysis. J. Res. NBS, Sect. A, v. 69A, 1965, pp. 237-243.
10. Levin, E. M., and R. L. Roth. Polymorphism of Bismuth Sesquioxide. I. Pure  $\text{Bi}_2\text{O}_3$ . J. Res. NBS, Sect. A, v. 68A, 1964, pp. 189-195.
11. Mah, A. D. Heats of Formation of Cerium Sesquioxide and Bismuth Sesquioxide by Combustion Calorimetry. BuMines RI 5676, 1961, 7 pp.
12. Mehrotra, G. M., M. G. Frohberg, and M. L. Kapoor. Standard Free Energy of Formation of  $\text{Bi}_2\text{O}_3$ . Phys. Chem. Neue Folge, v. 99, 1976, pp. 304-307.
13. Rao, A. V. R., and V. B. Tare. Free Energy of Formation of  $\text{Bi}_2\text{O}_3$ . Scr. Metall., v. 5, 1971, pp. 807-812.
14. Siderov, L. N., I. I. Minayeva, E. Z. Zasorin, I. D. Sorokin, and A. Ya. Borshevskiy. Mass Spectrometric Investigation of Gas-Phase Equilibria Over Bismuth Trioxide. High Temp. Sci., v. 12, 1980, pp. 175-196.
15. Humphrey, G. L., and C. J. O'Brien. Heats of Formation of Stannic and Stannous Oxides From Combustion Calorimetry. J. Am. Chem. Soc., v. 75, 1953, pp. 2805-2807.

16. Lavut, E. G., B. I. Timofeyev, V. M. Yuldasheva, E. A. Lavut, and G. L. Galchenko. Enthalpies of Formation of Tin (IV) and Tin (II) Oxides From Combustion Calorimetry. *J. Chem. Thermodyn.*, v. 13, 1981, 635-646.
17. Platteeuv, J. C., and G. Meyer. The System Tin + Oxygen. *Trans. Faraday Soc.*, v. 52, 1956, pp. 1066-1073.
18. Bedford, T. N., and C. B. Alcock. Thermodynamics and Solubility of Oxygen in Liquid Metals From EMF Measurements Involving Solid Electrolytes. *Trans. Faraday Soc.*, v. 61, 1965, pp. 443-453.
19. Petot-Ervas, G., R. Farhi, and C. Petot. Standard Gibbs Free Energy of Formation of  $\text{SnO}_2$  From High-Temperature E.M.F. Measurements. *J. Chem. Thermodyn.*, v. 7, 1975, pp. 1131-1136.
20. Ramanarayanan, T. A., and A. K. Bar. Electrochemical Determination of the Free Energy of Formation of  $\text{SnO}_2$ . *Metall. Trans. B*, v. 9B, 1978, pp. 485-486.
21. Seetharaman, S., and L. I. Steffanssen. On the Standard Gibbs Energy of Formation of  $\text{SnO}_2$ . *Scand. J. Metall.* v. 6, 1977, pp. 143-144.
22. Kiukkola, K., and C. Wagner. Measurements on Galvanic Cells Involving Solid Electrolytes. *J. Electrochem. Soc.*, v. 104, 1957, pp. 379-387.
23. Steel, B. C. H., and C. B. Alcock. Factors Influencing the Performance of Solid Oxide Electrolytes in High-Temperature Thermodynamic Measurements. *Trans. Metall. Soc. AIME*, v. 233, 1965, pp. 1359-1367.
24. Schaefer, S. C. Electrochemical Determination of the Gibbs Energy of Formation of Sphalerite ( $\text{ZnS}$ ). *BuMines RI 8301*, 1978, 16 pp.
25. Kofstad, P. Nonstoichiometry, Diffusion, and Electrical Conductivity in Binary Oxides. Wiley-Interscience, 1972, p. 355.
26. Pankratz, L. B. Thermodynamic Properties of Elements and Oxides. *BuMines B 672*, 1982, 509 pp.
27. Pastorek, R. L., and R. A. Rapp. The Solubility and Diffusivity of Oxygen in Solid Copper From Electrochemical Measurements. *Trans. Metall. Soc. AIME*, v. 245, 1969, pp. 1711-1720.
28. Das, S. K., and A. Ghosh. Thermodynamic Measurements in Molten Pb-Sn Alloys. *Metall. Trans.*, v. 3, 1972, pp. 803-806.
29. Ramanarayanan, T. A., and R. A. Rapp. The Diffusivity and Solubility of Oxygen in Liquid Tin and Solid Silver and the Diffusivity of Oxygen in Solid Nickel. *Metall. Trans.*, v. 3, 1972, pp. 3239-3246.